Determination of the Extent of DNA Bending by an Adenine–Thymine Tract†

Hyeon-Sook Koo, Jacqueline Drak, Janet A. Rice, and Donald M. Crothers*
Department of Chemistry, Yale University, New Haven, Connecticut 06511
Received December 18, 1989

ABSTRACT: We determined the magnitude of the bend induced in DNA by an adenine–thymine tract by measuring the rate of cyclization of DNA oligonucleotides containing phased A tracts. A series of linear multimers with 2-bp single-stranded ends, in which the $(A{\cdot}T)_6$ tracts are separated by $CG_{2-3}C$ sequences and are positioned 10 and 11 bp apart alternately, were prepared from 21 bp long synthetic duplexed deoxyoligonucleotides. The cyclization rates of the multimers (105–210 bp) and the bimolecular association rate of the 84 bp long multimer were measured in the presence of DNA ligase. From the rate constants of the cyclization and bimolecular association reactions, ring closure probabilities were obtained for the multimers. The systematically bent molecules were simulated by Monte Carlo methods, and the ring closure probabilities were calculated for a given set of junction bend angles. By comparing the calculated values of ring closure probabilities to experimental values and adjusting the junction bend angles to fit experimental values, the extent of bending at the junctions (or the extent of bending for an adenine tract) was determined. We conclude that an A_6 tract bends the DNA helix by 17–21°.

There are now several models to describe DNA bending by adenine–thymine tracts. In the junction bending model used by our laboratory (Levene & Crothers, 1983; Wu & Crothers, 1984; Koo et al., 1986; Koo & Crothers, 1988), bends are arbitrarily associated with the junction between adenine tracts and adjacent B-DNA. Analysis of symmetry properties and overall bend direction leads to assignment of bends primarily in the direction of tilt toward the T base at the 5′ junction of A tracts and toward the A base at the 3′ junction (Koo & Crothers, 1988; Zinkel & Crothers, 1987). In the wedge model suggested by Trifonov and his colleagues (Ulanovsky et al., 1987), bending at each ApA dinucleotide step occurs by roll toward the minor groove and also by tilt toward the T base with the roll:tilt ratio of 3.5:1. Maroun and Olson (1988) and Calladine et al. (1988) have suggested that bends result from wedge angles between adjacent bases in the non-A-tract region of the sequence. Insertion of straight A tracts between the B-DNA segments is the source of overall bending in this model. In spite of crystallographic analysis of A-tract-containing molecules (Nelson et al., 1987; Coll et al., 1987; DiGabriele et al., 1989), the origin of bending cannot be definitely stated at this time, since the direction of bending in the crystal does not conform to the results in solution (Koo & Crothers, 1988), nor are critical proton–proton distances found to be in good agreement when NMR results are compared with the crystal structure (Nadeau & Crothers, 1989). Furthermore, DiGabriele et al. (1989) showed that bending of the molecule in the crystal is determined primarily by crystal packing forces rather than by the sequence.

There have been only a few attempts to estimate extent of bending for DNA fragments containing A tracts. Hagerman (1984) measured the electric birefringence rotational relaxation time of a palindromic kinetoplast DNA fragment (242 bp) containing two bending loci. The curvature of the DNA fragment was estimated to be equivalent to a 52° bend at the center of the fragment. Levene et al. (1986) measured the rotational relaxation time for a kinetoplast DNA fragment (240 bp) by electric dichroism. By fitting the measured value with theoretical values calculated by using Monte Carlo methods, a bend angle of 9.0° at each junction (18° for an adenine tract) was obtained. The application of the junction bend angle (9°) to the kinetoplast DNA fragment studied by Hagerman predicts a 2-fold larger extent of bending than obtained from Hagerman's estimate for the DNA fragment. A different approach to measure the bend angle for an A tract (or for an ApA dinucleotide) was reported by Ulanovsky et al. (1986). A synthetic duplexed oligonucleotide (21 bp) containing A_5 and A_6 tracts separated by 10.5 bp was ligated into a series of multimers by DNA ligase. By analysis of the ratios of circular and linear multimers in the ligation product, the optimum size for cyclization was found to be 137 bp. However, these measurements do not measure cyclization kinetics directly and are uncorrected for (synthetic) DNA molecules with defective ends remaining in the linear products. From the optimum cyclization size, a bend of 8.7° at each ApA step (or a 28° bend per A tract) was calculated. The analysis of electrophoretic mobilities by Calladine et al. (1988) leads to a bend of about 11° per A tract. The measured bend angles in all studies combined range from 4.5° to 14° at each junction in terms of the junction bending model (9–28° per A tract), and the equivalent range of the ApA wedge angle is 2.5–8.7°.

To estimate the extent of bending by an A tract, we have measured cyclization kinetics to determine ring closure probabilities of DNA molecules containing A tracts. The ring closure probability (J factor) is defined as the ratio $J = K_c/K_a$ of the equilibrium constant for cyclization to that for bimolecular association (Shore et al., 1981; Shore & Baldwin, 1983). The J factor depends on the concentration of one end of a DNA molecule near the other end, the angular orientations between the two ends, and the twist angle between the two ends, which is a function of the DNA length and the helix screw. For systematically bent DNA molecules, the first two factors favor ring closure more than is the case for linear molecules, producing larger J factors for such molecules. This has been already shown in the calculated torsion angle independent ring closure probability (J_1) for a kinetoplast DNA fragment (240 bp) (Levene & Crothers, 1986a). The J_1 value computed by Monte Carlo simulation with an ApA bend angle

†Supported by Grant GM21966 from the National Institutes of Health.

0006-2960/90/0429-4227$02.50/0

of 5° is 2 orders of magnitude larger for a kinetoplast DNA fragment than for a straight DNA fragment of the same length.

As shown in the work by Shore et al. (1981, 1983), the J factors can be obtained experimentally by measuring the rate constants for cyclization and bimolecular association and taking the ratio of the two rate constants. This can be done provided that the fraction f_s of DNA molecules that are substrates for cyclization by ligase is smaller than about 0.1, allowing one to neglect the term $(1 - f_s)$ in eq 1, derived by Shore and Baldwin (1983):

$$k_1/k_2 = K_c(1 - f_s)/K_a(1 - f_s')^2 \quad (1)$$

Here k_1 and k_2 are the rate constants of the cyclization and bimolecular association reactions, K_c is the cyclization equilibrium constant, and K_a is the bimolecular equilibrium constant for the joining of two molecules. f_s' represents the fraction of DNA molecules that are substrates for dimerization by ligase. Under our experimental conditions the total DNA concentration (1.05×10^{-8} M) and the value of K_a (see below) are such that $f_s' \leq 1.0 \times 10^{-4}$. Neglect of this small value of f_s', using $K_c = f_s/(1 + f_s)$, allows eq 1 to be rearranged to

$$f_s = (k_1/k_2)K_a \quad (2)$$

Note that this equation implies an upper limit of $1/K_a$ on k_1/k_2 as $f_s \rightarrow 1$; as this limit is approached, $J = K_c/K_a$ becomes very different from k_1/k_2.

We have examined the validity of the assumption that $f_s \leq 0.1$ by determining an upper limit for K_a from temperature jump experiments performed with molecules analogous to those used in the bimolecular association experiments. This limit on K_a was then used to estimate a corresponding upper bound on f_s by using the experimental ratio k_1/k_2 and eq 2.

In this study, we measured k_1 and k_2 for DNA molecules in which A_6 tracts are repeated at 10- and 11-bp distances alternately. A 21-bp repeat was chosen because our earlier measurements (Koo et al., 1986) indicated that the helical repeat in A-tract-containing molecules is between 10 and 11 bp. Cyclization rates are dramatically increased in molecules containing a 21-bp repeat, compared to 10- or 11-bp repeats. The linear DNA substrates are multimers (4-mer–10-mer) of synthetic duplexed oligonucleotides (21 bp) containing two A_6 tracts. The bimolecular ligation rate constant was measured for the 4-mer, which is too short to cyclize. Since the bimolecular association rate constant was shown by Shore et al. (1981) to be independent of DNA size, the bimolecular rate constant of the 4-mer can be used in all the calculations of the ring closure probabilities for the multimers (5-mer–10-mer).

Levene and Crothers (1986a,b) calculated ring closure probabilities for random sequences of different length by Monte Carlo simulation. Using a closely related program, we calculated theoretical ring closure probabilities for the series of multimers at varying junction bend angles. In this process, the directions and relative magnitudes of the junction bends (5′ junction bend vs 3′ junction bend and tilt vs roll at each junction) were kept constant, as determined from the gel mobility data for bent DNA molecules of various sequences (Koo & Crothers, 1988). The magnitude of the overall bend was determined by fitting the calculated ring closure probabilities to experimental values for the series of multimers.

Materials and Methods

Preparation of Linear Multimers of the 21-bp Bent Sequence. The profile of preparation of linear multimers is illustrated in Figure 1. Chemically synthesized monomer A and monomer B both have two A tracts in 21 bp, and the only difference between the two monomers is the sequence between the two A tracts, as shown in Table I. Only monomer B has an *Msp*I site that can be used later to linearize circular molecules containing the monomer. Monomer A and monomer B were labeled with cold ATP and radioactive [γ-^{32}P]-ATP, respectively. They were mixed together in 5:1 (A:B) ratio and ligated into multimers. The ligated products contained mostly circular molecules, and those containing at least one copy of monomer B were linearized by *Msp*I digestion. The circular molecules containing copies of only monomer A were not linearized by the digestion. Since those molecules were not radioactive, they did not interfere in the subsequent separation of linearized multimers by gel electrophoresis and autoradiography. The experimental procedures are described below in detail.

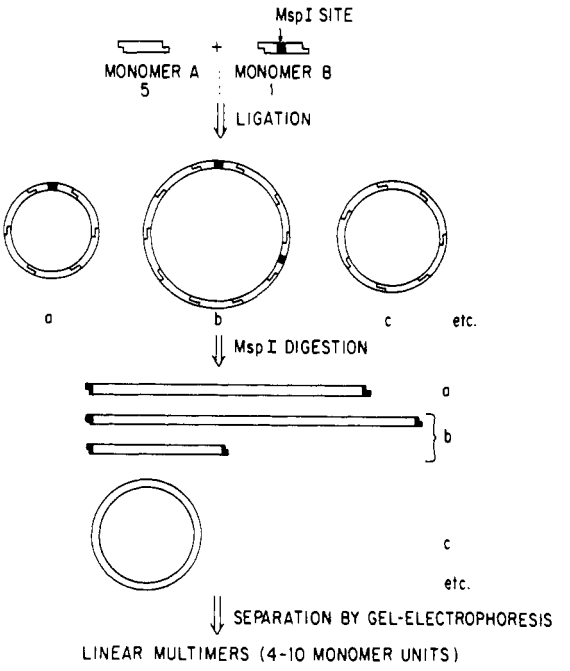

FIGURE 1: Preparation scheme for linear multimers of the 21-bp bent sequence. The sequences of monomers A and B are shown in Table I. The monomers have 5 bp long sticky ends and two A_6 tracts in 21 bp. Only monomer B was labeled radioactive; thus, the circular molecule C consisting of only monomers A was nonradioactive and did not interfere in the subsequent separation of linear multimers.

Table I: Synthetic Duplexed Oligonucleotides

```
Monomer A:  5′ GGGCAAAAAACGGCAAAAAAC
                TTTTTGCCGTTTTTTGCCCGT

                     Msp I Site
                         ↓
Monomer B:  5′ GGGCAAAAAACCGGAAAAAAC
                TTTTTGGCCTTTTTTGCCCGT

Molecule C: 5′ GGGCAAAAAACCGGAAAAAAC
                CCCGTTTTTTGGCCTTTTTTGGC
```

The oligonucleotide strands of monomer A and B were made on a DNA synthesizer (Applied Biosystems) and then purified on denaturing 20% polyacrylamide gels as described in the paper by Koo et al. (1986). For each monomer, the complementary strands were mixed and then hybridized by cooling slowly from 70 to 20 °C. The duplexed monomer A (8 μg) was phosphorylated with cold ATP (0.6 mM) and 20 units

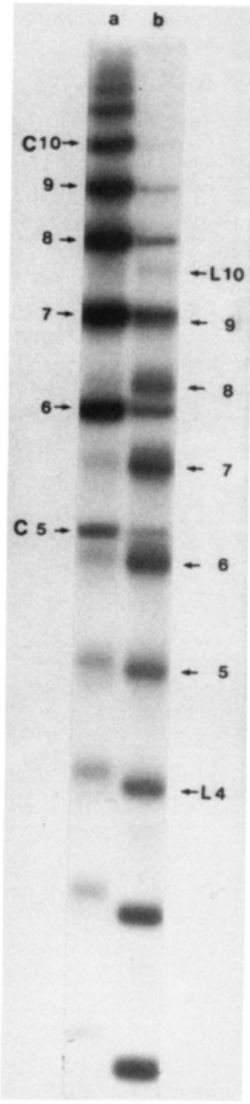

FIGURE 2: Autoradiogram of a native 6% polyacrylamide gel. (Lane a) Ligation products of the mixture of monomers A and B. (Lane b) After the *Msp*I digestion of the ligation products. The shape, circular (C) or linear (L), and length of the multimers were identified by using the method described by Ulanovsky et al. (1986). The number next to each band stands for the number of monomer copies in the multimer molecule.

of polynucleotide kinase (New England Biolabs) in a 50-μL volume at 37 °C for 30 min. The reaction was quenched by adding EDTA to a final concentration of 25 mM. The kinasing solution contained 70 mM Tris·HCl (pH 7.6), 10 mM $MgCl_2$, and 5 mM dithiothreitol. Hybridized monomer B (1.6 μg) was phosphorylated with 1 mCi of [γ-^{32}P]ATP (Amersham, 5 mCi/nmol) and 10 units of kinase in 50 μL of solution for 30 min. After monomer B was labeled with [γ-^{32}P]ATP, 3 μL of 1 mM cold ATP and an additional 10 units of kinase were added; the reaction was allowed to proceed for another 30 min and then quenched by adding EDTA. The solutions of phosphorylated monomers A and B were mixed together. Following phenol extraction and ethanol precipitation, the pellet of oligonucleotide duplexes was resuspended in a 38-μL solution containing the same constituents as in the kinasing buffer and 1 mM ATP. Two microliters of DNA ligase (New England Biolabs, 400 units/μL) were added, and the ligation was allowed to proceed at 37 °C for a few hours. The ligated products are shown on the autoradiogram of a native 6% polyacrylamide gel in Figure 2a. Following ligation the DNA was phenol-extracted and ethanol-precipitated. The DNA pellet was resuspended in 100 μL of *Msp*I digestion buffer, and 100 units of *Msp*I restriction enzyme (New England Biolabs) was added. After *Msp*I digestion for several hours, the digested mixture was phenol-extracted and ethanol-precipitated.

To separate linear multimers of different lengths, the digested products were electrophoresed on a nondenaturing 6% polyacrylamide gel, as shown in Figure 2b. The gel was autoradiographed, and the bands of linear multimers (4-mer–10-mer) were excised from the gel. The DNA fragments in the gel slices were electroeluted, phenol-extracted, ethanol-precipitated, and resuspended in TE buffer. The amount of each multimer recovered from the gel slices was determined by measuring radioactive levels of the DNA samples as follows. A small fraction of [γ-^{32}P]ATP-labeled monomer B solution, which was later used to make the multimers, was electrophoresed on a native 4% polyacrylamide gel and separated from unreacted ATP and radioactive contaminants. The monomer B band was cut out of the gel, and the radioactivity level of the band was measured in a scintillation counter. From the known DNA concentration of the monomer B solution and the measured radioactivity level, the specific radioactivity (cpm/mole) of monomer B molecules was obtained. As illustrated in Figure 1, all radioactive linear multimers have half of a monomer B molecule at one end and the other half of a monomer B molecule at the other end of the molecule, corresponding to one molecule of monomer B per multimer molecule. Therefore, all linear multimers have the same specific radioactivities as monomer B. From the specific radioactivities and measured radioactivity levels of the linear multimers, absolute amounts of the linear multimers recovered from the gel slices were determined.

Preparation of the Molecules for the Relaxation Experiments. The oligonucleotide strands of molecule C (see Table I) were made on a DNA synthesizer (Applied Biosystems) and then purified on a 20% polyacrylamide gel, 39:1 acrylamide:Bis, 50% urea. The DNA strands were visualized by UV shadowing, excised from the gel, and electroeluted into 1/2× TBE (49 mM Tris-HCl, pH 8.0, 1 mM EDTA) for 12 h at 50 V. The eluates were collected and dialyzed against 10 mM Tris-HCl, pH 7.6, for 24 h, with three changes of dialysis buffer. The samples were then concentrated to one-fifth of their original volume so that the final Tris concentration was 50 mM. The monomer strands were annealed by heating to 75 °C and cooling slowly to 18 °C. The final duplex concentration was 1.67×10^{-5} M in a solution containing 50 mM Tris-HCl, pH 7.6, and 50 mM Na_2SO_4.

Cyclization Kinetics. Cyclization rates were measured for each linear multimer (5-mer–10-mer) at 22 °C at the initial concentration of linear multimers of 1.0×10^{-9} M. The reaction solution contained 50 mM Tris-HCl (pH 7.6), 10 mM $MgCl_2$, 10 mM DTT, 1 mM ATP, and BSA (100 μg/mL). T4 DNA ligase (New England Biolabs, 400 units/μL, specific activity = 9.5×10^5 units/mg) was diluted to a concentration of 0.2 units/μL with buffer containing 50 mM KCl, 10 mM Tris-HCl (pH 7.6), 0.1 mM EDTA, 1 mM DTT, 200 μg/mL BSA, and 10% glycerol. From the original reaction volume of 120 μL, an 8-μL sample was withdrawn for a zero-time point, and then 6 μL of the diluted ligase (0.2 units/μL) was added to the reaction mixture to a final concentration of ligase of 1.7×10^{-10} M. The reaction solution was mixed manually, and aliquots of 8 μL were withdrawn every 30 s for 5 min. The aliquots were mixed with 8 μL of 50 mM EDTA solution to quench the reaction. Then the aliquots were electrophoresed on either 4% or 6% native polyacrylamide gels depending on

the size of the DNA fragments. The gels were autoradiographed, and the linear and circular DNA bands were cut out of the gel. Radioactivity levels of the bands were measured in a scintillation counter.

Bimolecular Association Kinetics. The 4-mer of the bent sequence was used as a substrate for the bimolecular association reaction, since it cannot cyclize directly. At the concentrations of DNA substrate and ligase used in the cyclization kinetic studies, neither cyclized nor dimerized products of the 4-mer molecules were detected after 10 min of ligation. Therefore, higher concentrations of DNA substrate and ligase were necessary to obtain detectable amounts of bimolecular ligation products. Except for the concentrations of DNA substrate and ligase, other reaction conditions and procedures were the same as in the cyclization rate measurements. The concentrations of DNA substrate and ligase were 1.05×10^{-8} and 8.5×10^{-9} M, respectively. Corrections necessitated by this procedure are discussed below.

Temperature Jump Measurements. The relaxation kinetics of the dimerization reaction was monitored at 256, 283, and 301 nm in the *T* jump apparatus described previously (Cole et al., 1972). The temperature before the jump was 22.5 ± 0.5 °C. The sample buffer was 50 mM Tris-HCl, pH 7.6, and 50 mM Na_2SO_4.

Theory and Calculations

Theory. We used the algorithm of Levene and Crothers (1983) for simulating the conformations of DNA. We treat the DNA molecule as a discrete wormlike chain in which each base pair is represented by a vector normal to the mean plane of the base pair. Propeller twisting or other deformations of the bases out of a plane perpendicular to the helix axis are ignored in this realization of the DNA molecule. Thermal motion is modeled by allowing the orientation of the helix axis to fluctuate through random small rotations about the *x*, *y*, and *z* axes at each base pair treated independently. The angles are chosen by assuming a Hooke's law restoring force for deviations from the mean angle and result in a Gaussian distribution of possible configurations.

As shown by Levene and Crothers (1983), the probability density that a base pair will be rotated with respect to its neighbor by angles θ, ϕ, and τ about the *x*, *y*, and *z* axes is $f(\theta,\phi)f(\tau)$, where

$$f(\theta,\phi) = c' \exp\left\{-\left[\frac{(\theta-\theta_0)^2}{2\sigma_\theta^2} + \frac{(\phi-\phi_0)^2}{2\sigma_\phi^2}\right]\right\}$$

$$f(\tau) = c'' \exp\left\{-\left[\frac{(\tau-\tau_0)^2}{2\sigma_\tau^2}\right]\right\}$$

The angles θ_0, ϕ_0, and τ_0 represent both the mean values for roll, tilt, and twist of the two adjacent base pairs with respect to each other and also the perfect helix parameters. c' and c'' are normalization constants; σ_θ and σ_ϕ are chosen such that $\sigma_\theta^2 + \sigma_\phi^2 = 2l/P$, where l is the helix rise per base pair and P is the persistence length of the DNA (Shellman, 1974). Thermal bending is assumed to have no preferred direction, and the DNA is treated as an isotropic chain where σ_θ is equal to σ_ϕ. In the torsion angle distribution, $(\sigma_\tau)^2 = lk_BT/C$, where k_B is Boltzman's constant, T is the absolute temperature, and C, the torsional modulus, is taken as 3.4×10^{-19} erg cm (Levene & Crothers, 1986b). All angular standard deviations are in terms of radians per base pair.

The original computer program to calculate the *J* factors was written by Levene and Crothers (1986a,b) and was based on earlier work by Jacobson and Stockmayer (1950) and Flory et al. (1976). They show that

$$J = 4\pi W(0)\Gamma_0(1)\Phi_{0,1}(\tau_0)/N_{AV}$$

in which the function $W(R)$ is the probability density for the end-to-end distance R and $\Gamma_R(\gamma)$ is the conditional probability density for the scalar product γ of the terminal chain vectors with the value of R specified. $\Phi_{R,\gamma}(\tau)$ is the conditional probability density for the torsional angle τ between the terminal chain vectors with R and γ specified, and N_{AV} is Avogadro's number.

Calculation Methods. The base sequence chosen is shown in Table I and corresponds to the experimental sequence. In this particular base sequence, the A_n bending unit is as close to in phase with the helical screw as is possible for DNA oligomers containing two helical turns. Multimers of the 21 base pair sequence were generated by tandem repetition to probe the variation of *J* with DNA chain length. Computer simulations were carried out on a VAXserver 3500 or on a VAXstation 3200 using code written in FORTRAN 77 modified from the original code written by Levene and Crothers (1986a,b). To describe the closure reaction of the DNA chain, an ensemble of systematically bent DNA chains was filtered to meet the cyclic boundary conditions.

For these calculations the DNA was represented as by Levene and Crothers (1983) with a series of coordinate systems each positioned such that the helix axis corresponds to the *z* axis of the local coordinate frame and the *x*–*y* plane corresponds to the mean base pair plane. Repeated application of standard rotation matrices generates a trajectory for the helix axis (Levene & Crothers, 1983). Random number generators were used to sample the Gaussian distributions used for the angles θ, ϕ, and τ. Computation time was minimized through the use of two subchains, each composed of half the number of base pairs in the original DNA chain. Each subchain in one of the sets was paired with all the subchains in the other set to generate an ensemble of full-length chains.

The root mean square end-to-end distance was computed for each chain and a radial distribution function for the ensemble of chains generated. The final values of the end-to-end distance and relative rotation about the *x* and *y* axes for the two terminal base pairs were used to filter chains for compliance with closed circle boundary conditions. The three constraints that specify closed circle boundary conditions are applied sequentially. An end-to-end distance cutoff, R_c, is established, and chains whose end-to-end distances fall outside R_c are discarded. For the remaining chains, the relative orientation of the initial and final vectors representing the helix axis is tested by obtaining the scalar product of the two vectors. Those chains in which the ends are nearly parallel (with scalar product greater than the angular cutoff γ_c) are retained and accumulated in a 100-point histogram corresponding to the angular distribution function, and those with $\gamma \leq \gamma_c$ are rejected. The angle between the initial and final *x* vectors corresponds to the torsional angular distribution function and is accumulated in a 72-point histogram. The ring closure probability was calculated by reexpressing the distribution functions as volume distribution functions and then extrapolating all the distributions to perfect alignment by using least-squares methodology to fit the experimental curves to even fourth-order polynomials.

The calculations were used to refine the magnitude of the angular parameters of the junction bending model for systematic bending of DNA at the junctions between homologous runs of dA·dT and random sequence B-DNA. It is important to stress that these simulations involve other parameters as

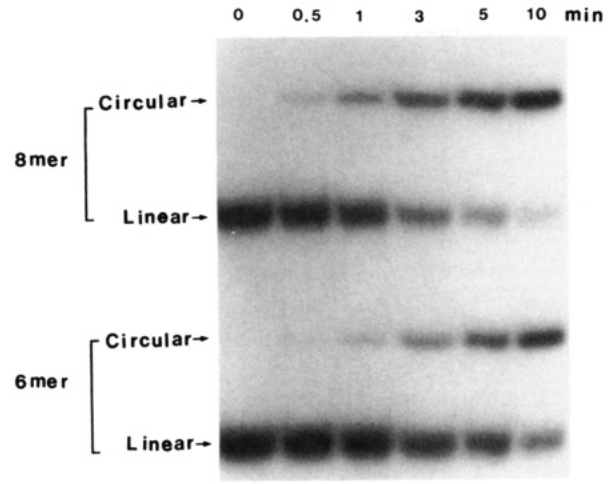

FIGURE 3: Cyclization kinetics shown on a native 4% polyacrylamide gel. The linear 6-mer and 8-mer were mixed and then cyclized in the same reaction tube to make sure that reaction conditions were identical for the two multimers. During this assay, the concentrations of each multimer and ligase were 1.0×10^{-9} and 2.5×10^{-10} M, respectively. However, the cyclization rate constant used for the J factor calculation was measured for each multimer separately.

well: the results will depend not only on the values for the bend angles but also on the helical repeat and the thermal bending flexibility of these sequences. To reduce the number of parameters, we have determined the helical screw of A_n tracts embedded in B-DNA in a separate, independent experiment (J.D. and D.M.C., unpublished results); we found a value of 10.35 ± 0.04 bp/turn, which was used as a starting point for the simulations. After obtaining a range of angular parameters that gave a reasonable fit with the experimental J values, we also studied the effect of modifying the chain's flexibility by varying the values of σ_θ and σ_ϕ up to 15% of the original value.

The angular parameters for B-DNA were chosen as $\theta_o = \phi_o = 0$. The ratios of θ (roll) to ϕ (tilt) at the 5′ and 3′ junctions of the A_n tract with B-DNA were chosen so that they correctly predict the observed anomalous gel mobilities found for bent DNA molecules of various sequences (Koo & Crothers, 1988). A persistence length of 475 Å was used for both the A_n tract and B forms of DNA (Levene & Crothers, 1986a). The cutoff value of the end-to-end distance (R_c) was 6 bp, and the critical value for angular orientation (γ_c) was 0.9. The number of subchains generated in each calculation was 10000, yielding a total of 10^8 chains in the ensemble.

Results

Cyclization Rate Measurements. For comparison, the cyclization kinetics of the 6-mer and the 8-mer are shown on the autoradiogram of a native 4% polyacrylamide gel in Figure 3. It can be easily seen that the 8-mer cyclizes about twice as fast as the 6-mer. No products of bimolecular association were detected at the concentration of substrates used here. From the measured levels of linear and circular DNA bands, the cyclized fractions of DNA molecules $\{1 - ([D_t]/[D_0])\}$ were calculated for each reaction time: $[D_t]$ is the concentration of remaining reactants at time t. In Figure 4, cyclized fractions are plotted against reaction time for the multimers of different length. Because cyclization is a first-order reaction, the plots of $\ln([D_t]/[D_0])$ against reaction time are linear. Cyclization rate constants (k_1) for the multimers were obtained from the slopes of the corresponding plots.

Bimolecular Association Rate Measurements. In the bimolecular association reaction of the 4-mer, the concentrations of the DNA reactant and ligase were higher than in the cyclization reactions. The 4-mer does not cyclize but instead dimerizes slowly to form the linear 8-mer, which is quickly converted to circular form. Even at the high concentrations of ligase and reactant, only a small fraction of the reactant is converted to products. Radioactive levels of the product, circular 8-mer, are so low that this resulted in a relatively large error in the bimolecular association rate measurements. The kinetic curve of the bimolecular association is plotted in Figure 5. The best-fit line for the data points in Figure 5 does not go through the origin, indicating faster kinetics in the first minute of the reaction than later. The slope of the best-fit line is $([D_0] - [D_t])/([D_0]t) = 1.0 \times 10^{-5}$ s^{-1}. From the slope and the initial concentration of the reactant, the second-order reaction rate constant was calculated: $k_2' = 9.5 \times 10^2$ M^{-1} s^{-1}.

The DNA reactant molecules have 5′CG unpaired bases at both ends of the molecule. In the bimolecular association of two molecules with two reaction sites per molecule, there are four possible ways of association. Thus, the rate of bimolecular

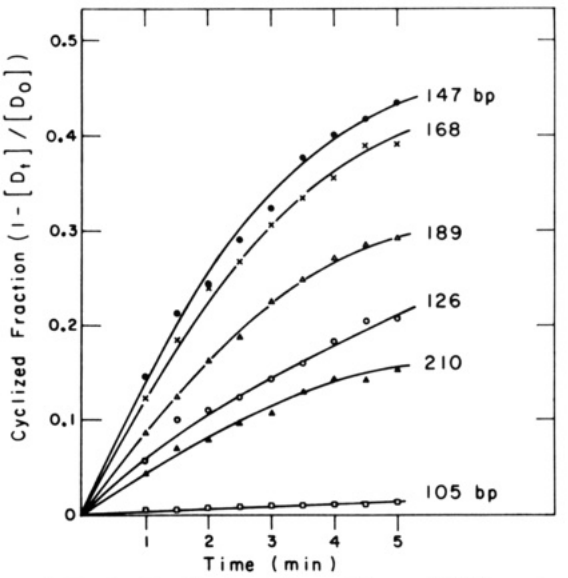

FIGURE 4: Cyclization kinetics of the multimers of different length. The concentrations of the reactants and ligase were 1.0×10^{-9} and 1.7×10^{-10} M, respectively. Only for the 105 bp long multimer was a higher ligase concentration (1.7×10^{-9} M) used, because the cyclization rate of the 5-mer was too low to be measured experimentally otherwise. The measured cyclized fraction of the 5-mer was corrected for the different enzyme concentration. $[D_t]$ is the concentration of the remaining DNA reactant at time t.

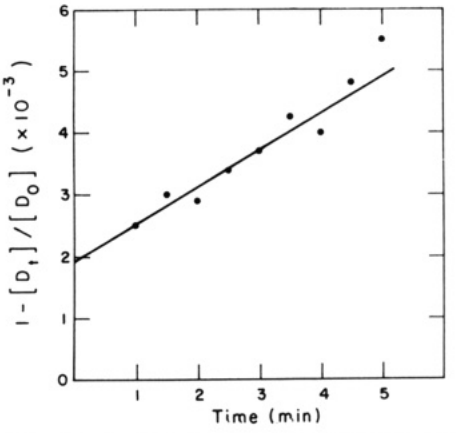

FIGURE 5: Bimolecular kinetics of the 4-mer (84 bp). The fraction of the dimerized product was plotted against the reaction time. From the slope and the initial concentration of the 4-mer, the second-order rate constant was obtained. The concentrations of the 4-mer and ligase were 1.05×10^{-8} and 8.5×10^{-9} M, respectively.

Table II: Cyclization Rate Constant k_1 ($\times 10^{-4}$ s^{-1}) of the 5-mer and 7-mer at Different Concentrations of the DNA Reactants and Ligase

[ligase] (10^{-10} M)	[5-mer] (10^{-9} M)		[7-mer] (10^{-9} M)	
	1.0	10	1.0	10
1.7			19.5	12.5
2.8		0.41		
8.5	2.18	1.46		
28.		3.75		
85.	11.8	7.87		

Table III: A-Tract Bend Angles According to the Junction Model[a]

symbol (Figure 6)	helical screw (bp/turn)	junction	tilt (deg)	roll (deg)	overall bend (deg)
■	10.35	5′	−7.7	4.6	18
		3′	9.7	0.0	

[a] A positive value of tilt means bending toward the strand that runs in the 5′-to-3′ direction (in this case, the strand with adenine tracts), and a positive value of roll means bending toward the major groove. The bend in the junction model is located in the coordinate frame of the first and last nucleotides of A tracts.

association of molecules with two reactive ends per molecule will be 4 times faster than that of molecules with one reactive end per molecule, at a given concentration of DNA molecules. The reaction rate constant should be divided by the degeneracy factor, 4, to obtain the real rate constant, $k_2 = 2.4 \times 10^2$ M^{-1} s^{-1}, needed for comparison with the cyclization experiments.

The concentrations of DNA reactant and ligase were 10 and 50 times higher, respectively, in the bimolecular association reaction than in the cyclization reactions. To calculate the J value, which is the ratio k_1/k_2, the measured rate constant k_2 needs to be corrected to a value valid at the same reaction conditions as in the cyclization reaction. In the derivation of the equations for the rate constants k_1 and k_2 by Shore et al. (1981, 1983), the cyclization rate and bimolecular association rate were expressed as a first- and second-order function of the DNA reactant concentration, respectively. The resultant rate constants k_1 and k_2 are both linear functions of the enzyme concentration, independent of the DNA reactant concentration. On the assumption that the measured rate constants obey this statement, the bimolecular rate constant k_2 at the enzyme concentration of the cyclization is obtained by correcting for the 50 times higher enzyme concentration: $k_2 = 4.8$ M^{-1} s^{-1}.

To correct for deviations from ideal dependence on enzyme and reactant concentrations, cyclization rates were measured at different concentrations of the 5-mer and ligase. As shown in Table II, when the ligase concentration was increased 3-fold from 2.8×10^{-10} to 8.5×10^{-10} M, the cyclization rate constant also increased about 3-fold, showing that the reaction rate is proportional to the ligase concentration within this range of ligase concentration. When the ligase concentration was further increased 10-fold (from 8.5×10^{-10} to 8.5×10^{-9} M), the cyclization rate constant was increased only about 5 times, showing a deviation from the linear relationship between the cyclization rate constant and ligase concentration. When the reactant concentration was increased 10 times from 1.0×10^{-9} to 1.0×10^{-8} M at the same ligase concentration, the cyclization rate constant decreased by 33%.

The K_m value of T4 DNA ligase is approximately 6.0×10^{-7} M as measured under the reaction conditions close to those used here (Raae et al., 1975; Sugino et al., 1977). The concentrations of the 5-mer and ligase in Table II are much lower than the K_m value. The dependence of the k_1 value on the DNA concentration is identical at the two different ligase concentrations (8.5×10^{-10} and 8.5×10^{-9} M). Although the 7-mer produces a much higher fraction of hybridized circular substrate for ligase, it has the same dependence of k_1 on DNA concentration as does the 5-mer. The observed deviations of the cyclization kinetics from ideal behavior can be ascribed to partial saturation due to enzyme binding to the DNA ends, formation of ligase aggregates, or inhibitory effects by nonsubstrate DNA.

We make the plausible assumption that the reaction rate constant in the bimolecular association has the same dependence on the concentration of reactant and enzyme as found in the cyclization reaction. The measured value $k_2 = 4.8$ M^{-1} s^{-1} was therefore corrected to a value $k_2 = 13.3$ M^{-1} s^{-1} by using the correction factors obtained from the cyclization reactions of the 5-mer.

Temperature Jump Measurements. We first attempted to measure the relaxation time using molecule C (see Table I), but no signal could be detected within the sensitivity of our experimental setup. When we used the same concentration of shorter molecules of comparable sequence with the same GC overhang, we observed a relaxation time (τ) corresponding to the dimerization reaction, with a signal-to-noise ratio ≥ 10. The relaxation curves were obtained for a series of concentrations, and a plot of $(1/\tau)^2$ versus DNA monomer concentration allowed us to determine $K_a = (8.0 \pm 2.0) \times 10^3$ M^{-1}. From the fact that we did not observe a signal for molecule C, we estimate that $K_a \leq 8 \times 10^2$ M^{-1}. This makes $f_s \leq 0.1$ so that we can approximate the cyclization factor as the ratio of the two rate constants. However, we emphasize that longer complementary ends may have association constants K_a which are large enough to require a correction for the value of f_s.

Fitting Procedure for Experimental and Theoretical J Factors. From the determined k_1 values for the series of multimers and the k_2 value for the 5-mer, J factors were calculated for the multimers. As shown in Figure 6, the J values for the multimers are much larger for bent sequences, compared to DNA fragments of random sequences ($J < 10^{-8}$ M) in the same range of length. The 7-mer (147 bp) and 8-mer (168 bp) are the two multimers of the largest J factors, and the optimum length for cyclization is approximately 155 bp (15 A tracts) between the two multimers. This yields a preliminary estimate of $360°/15 = 24°$ bending per A tract, which is refined to somewhat smaller values by the computer simulation experiments described below.

In the measurement of rate constants for the multimers, there is a relatively small experimental error (5%) in k_1 but significantly larger experimental error (25%) in k_2. In addition to the experimental errors, there could be a methodological error in correcting the k_2 value to the value corresponding to the reaction conditions used for k_1 measurements. Even though it is assumed for the correction that the dependence of k_2 on reactant and ligase concentrations is the same as that of k_1, this may not be entirely true. From the above considerations, there is a significant error in the k_2 value and consequently in the absolute magnitudes of the experimental J values. However, the distribution of J values with DNA length is thought to be quite reliable. In the fitting process, both the absolute magnitude of J values and their variation with DNA length were considered.

We first examined the effect of varying the overall bend angle, keeping the directions and relative magnitudes of the junction bends constant (5′ junction bend vs 3′ junction bend and tilt vs roll at each junction) and taking the helical screw as 10.35 bp/turn. The best fit to the experimental values was obtained for an overall bend angle of 18° per A_n tract (see Figure 6a and Table III). Smaller bend angles shift the maximum of the plot toward longer molecules and drastically reduce the J values for the shorter ones. Larger bend angles

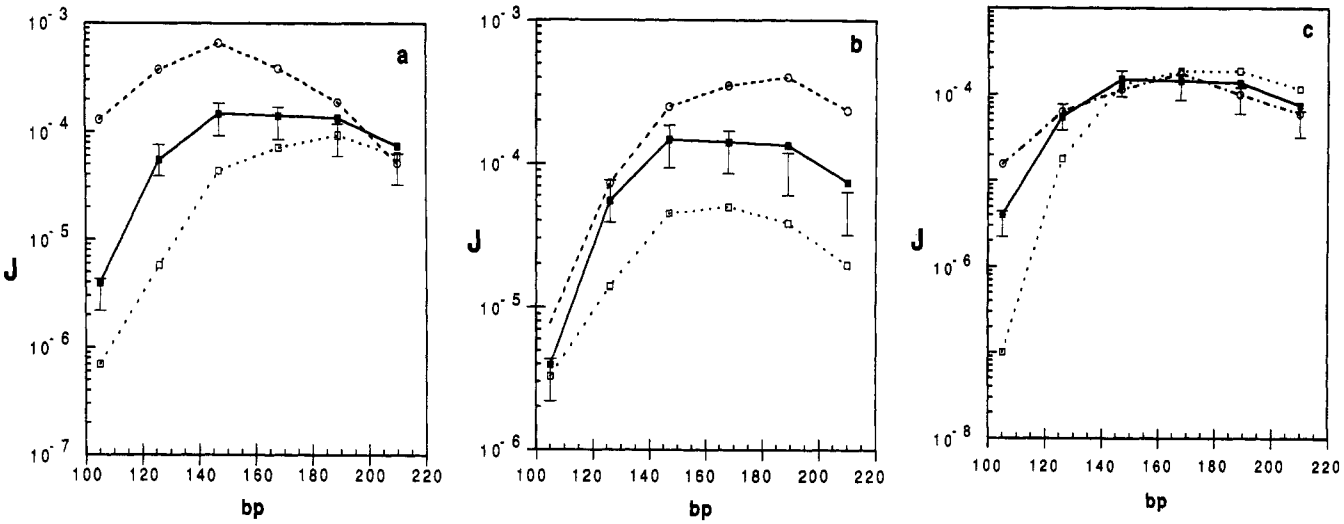

FIGURE 6: Comparison of the experimental J factors with the theoretical values for the multimers of various lengths. The experimental J factors are marked with error bars. (a) Effect of varying the overall bend angle on the theoretical J factor, using the experimentally determined helical repeat of 10.35 bp/turn (J. Drak and D. M. Crothers, unpublished results). The bend angles were (□) 16°, (■) 18°, and (○) 22°. (b) Effect on the theoretical J factor of varying the helical repeat for an overall bend angle of 18°; helical repeat values were (□) 10.30, (■) 10.35, and (○) 10.40. (c) Effect on the theoretical J factor of increasing (○) or decreasing (□) the thermal bending flexibility (σ_β,σ_ϕ) by 10%. The helical repeat is 10.35 bp/turn, and the bend angle is 18°. The J values obtained with the usual flexibility are indicated as ■.

tend to broaden the distribution of J values and also to make it more symmetric. For example, with a 22° bend angle, the 5-mer should cyclize as readily as the 9-mer, which is drastically different from what is observed experimentally.

We also wanted to study the effect of altering the helical repeat (h) while keeping the overall bend angle constant (18°). It is apparent that the calculations are extremely sensitive to the value of the helical screw (see Figure 6b). The best fit to the experimental data was obtained with h values ranging from 10.33 to 10.36 bp/turn. A relatively small increase in the helical repeat (from 10.35 to 10.4 bp/turn) shifts the maximum of the distribution of J values to longer molecules; on the other hand, reducing h from 10.35 to 10.3 bp/turn lowers the J factor for all the multimers. Larger deviations of the helical repeat from the optimum range follow the same trend.

The general effect of varying the chain flexibility in an isotropic manner is illustrated in Figure 6c. Decreasing the flexibility by 10% sharpens the distribution of J values and also shifts the maximum of the plot toward longer molecules. In contrast, increasing the flexibility by 10% broadens the distribution and has little effect on the position of the maximum.

Summarizing, then, the overall bend angle produced by an A_6 tract is calculated to be between 17° and 21°. It should be emphasized that this estimate of the bend angle does not distinguish among the detailed models proposed to describe bending, whether junction, wedge, or other as preferred. Any model that produces an overall bend of this magnitude is consistent with the data reported here.

Discussion

By adjusting calculated J values to experimental J values of the bent molecules, we estimate an overall bend angle per A tract of 17–21°. This range of bend angles, whose uncertainty derives largely from the multiparameter nature of these simulations and the experimental errors involved in our measurements, agrees with the estimate by Levene et al. (1986), 9.0° at each junction (18° overall), which was obtained from measurements of rotational relaxation times of kinetoplast DNA fragments. Hagerman's estimate (Hagerman, 1984) of the extent of bending for the palindromic kinetoplast DNA fragment is much smaller than our range of values, while the estimate by Ulanovsky et al. (1986) is larger than the bend angle determined here. The electron microscope observations of Griffith et al. (1986) are in good agreement with a bend angle of about 20° per A tract, since they found that molecules containing 18 A tracts appeared circular. The bend angle estimated by Calladine et al. (1988) is too small to be accommodated to our results. Their estimate refers to conditions in the gel, and ours to ligation conditions in solution, so the measurements are not strictly comparable. However, a 2-fold difference in curvature translates into a 4-fold change in magnitude of the gel anomaly (Koo & Crothers, 1988), so were there a strong dependence of bending on ionic conditions, one would expect it to be readily detectable by varying the gel buffer.

Our results illustrate the power of combining experimental measurements of cyclization kinetics with computer simulation of DNA chain mechanics to obtain precise estimates of chain parameters including bend angle, average helical repeat, and stiffness. An accurate value for the bend angle produced by A tracts, combined with knowledge of the bend direction, allows A tracts to be used as primary standards for comparative measurement of other bends (Rice et al., 1988; Rice & Crothers, 1989; Zinkel & Crothers, 1990).

Acknowledgments

We thank Karen LeCuyer for skillful assistance with the T jump experiments and Grace Sun for oligonucleotide synthesis.

References

Calladine, C. R., Drew, H. R., & McCall, M. J. (1988) *J. Mol. Biol. 201*, 127–137.

Cole, P. E., & Crothers, D. M. (1972) *Biochemistry 11*, 4368–4374.

Coll, M., Frederick, C. A., Wang, A. H.-J., & Rich, A. (1987) *Proc. Natl. Acad. Sci. U.S.A. 84*, 8385–8389.

Diekmann, S., & Wang, J. C. (1985) *J. Mol. Biol. 186*, 1–11.

DiGabriele, A. D., Sanderson, M. R., & Steitz, T. A. (1989) *Proc. Natl. Acad. Sci. U.S.A. 86*, 1816–1820.

Flory, P. J., Suter, U. W., & Mutter, M. (1976) *J. Am. Chem. Soc. 98*, 5733–5739.

Griffith, J., Bleyman, M., Rauch, C. A., Kitchin, P. A., & Englund, P. T. (1986) *Cell 46*, 717–724.
Hagerman, P. J. (1984) *Proc. Natl. Acad. Sci. U.S.A. 81*, 4632–4636.
Jacobson, H., & Stockmayer, W. H. (1950) *J. Chem. Phys. 18*, 1600–1606.
Koo, H.-S., & Crothers, D. M. (1988) *Proc. Natl. Acad. Sci. U.S.A. 85*, 1763–1767.
Koo, H.-S., Wu, H.-M., & Crothers, D. M. (1986) *Nature 320*, 501–506.
Levene, S. D., & Crothers, D. M. (1983) *J. Biomol. Struct. Dyn. 1*, 429–435.
Levene, S. D., & Crothers, D. M. (1986a) *J. Mol. Biol. 189*, 61–72.
Levene, S. D., & Crothers, D. M. (1986b) *J. Mol. Biol. 189*, 73–83.
Levene, S. D., Wu, H.-M., & Crothers, D. M. (1986) *Biochemistry 25*, 3988–3995.
Maroun, R. C., & Olson, W. K. (1988) *Biopolymers 27*, 585–603.
Nadeau, J. G., & Crothers, D. M. (1989) *Proc. Natl. Acad. Sci. U.S.A. 86*, 2622–2626.
Nelson, H. C. M., Finch, J. T., Luisi, B. A., & Klug, A. (1987) *Nature 330*, 221–226.
Raae, A. J., Kleppe, R. K., & Kleppe, K. (1975) *Eur. J. Biochem. 60*, 437–443.
Rice, J. A., & Crothers, D. M. (1989) *Biochemistry 28*, 4512–4516.
Rice, J. A., Crothers, D. M., Pinto, A. L., & Lippard, S. J. (1988) *Proc. Natl. Acad. Sci. U.S.A. 85*, 4158–4161.
Shellman, J. A. (1974) *Biopolymers 13*, 217–226.
Shore, D., & Baldwin, R. (1983) *J. Mol. Biol. 170*, 957–981.
Shore, D., Langowski, J., & Baldwin, R. (1981) *Proc. Natl. Acad. Sci. U.S.A. 78*, 4833–4837.
Sugino, A., Goodman, H. M., Heynecker, H. L., Shine, J., Boyer, H. W., & Cozarelli, N. R. (1977) *J. Biol. Chem. 252*, 3987–3994.
Ulanovsky, L., & Trifonov, E. N. (1987) *Nature 326*, 720–722.
Ulanovsky, L., Bodner, M., Trifonov, E. N., & Choder, M. (1986) *Proc. Natl. Acad. Sci. U.S.A. 83*, 862–866.
Wu, H.-M., & Crothers, D. M. (1984) *Nature 308*, 509–513.
Zinkel, S. S., & Crothers, D. M. (1987) *Nature 328*, 178–181.
Zinkel, S. S., & Crothers, D. M. (1990) *Biopolymers 29*, 29–38.